




Span shift and extension of quantum microwave electrometry with Rydberg atoms dressed by an auxiliary microwave field

Feng-Dong Jia,¹ Xiu-Bin Liu,¹ Jiong Mei,¹ Yong-Hong Yu,^{1,2} Huai-Yu Zhang ,¹ Zhao-Qing Lin ,¹ Hai-Yue Dong,¹ Jian Zhang,³ Feng Xie ^{3,*} and Zhi-Ping Zhong^{1,4,†}

¹*School of Physical Sciences, University of Chinese Academy of Sciences, Beijing 100049, China*

²*Institute of Physics, Chinese Academy of Sciences, Beijing 100190, China*

³*Institute of Nuclear and New Energy Technology, Collaborative Innovation Center of Advanced Nuclear Energy Technology, Key Laboratory of Advanced Reactor Engineering and Safety of Ministry of Education, Tsinghua University, Beijing 100084, China*

⁴*CAS Center for Excellence in Topological Quantum Computation, University of Chinese Academy of Sciences, Beijing 100190, China*



(Received 12 January 2021; revised 6 April 2021; accepted 8 June 2021; published 24 June 2021)

The Rydberg electromagnetically induced transparency (EIT)–Autler Townes (AT) splitting proportional to the target microwave electric field strength is an atom-based primary traceable standard in microwave electrometry. The minimum detected microwave electric field is limited when the EIT-AT splitting is indistinguishable. We design a method for auxiliary microwave-dressed Rydberg atoms that extends the electrometric span. We theoretically and experimentally show that the low bound of the direct SI-traceable microwave electric field is extended by two orders of magnitude, which is from several mV/cm to μ V/cm in a room-temperature Rb cell with a modest setup.

DOI: [10.1103/PhysRevA.103.063113](https://doi.org/10.1103/PhysRevA.103.063113)

I. INTRODUCTION

Quantum sensors [1] employ quantum-mechanical systems for measuring various physical quantities, ranging from time and frequency [2,3] to magnetic and electric fields [4–6], temperature, and pressure [7]. Quantum sensors have become a distinct and rapidly growing branch of research in quantum science and engineering in recent decades. An ideal quantum sensor is expected to provide a strong response only to the target physical quantity, and the observed signal has a monotonic relationship with the target physical quantity [1]. Owing to advantages such as reproducibility, accuracy, and stability, many quantum-system-based measurement techniques are adopted as direct International System of Units (SI) traceability paths. A setup of Rydberg atoms in a vapor cell with bright resonance has attracted steady research interest as a candidate for a primary traceable standard for microwave electrometry [8]. The Rydberg electromagnetically induced transparency (EIT) Autler-Townes (AT) splitting is proportional to the target microwave electric field strength in the AT regime [8–10]. The detection of weak microwave fields is important for many practical applications. The lower limit of the AT regime corresponds to the lower bound of the direct SI-traceable microwave electric field, which has been reported previously as approximately 5 mV/cm in room-temperature vapor cells [8–10]. Simons *et al.* varied the microwave (MW) frequency from resonance to detuning to extend the interval of EIT-AT splitting under the same MW electric field strength [11] as $\Delta f_m = \sqrt{(\delta_{MW})^2 + (\Delta f_0)^2}$, where δ_{MW} is the MW

detuning and Δf_0 is the separation of the two peaks with no rf detuning (or when $\delta_{MW} = 0$). Their MW detuning approach is able to measure an MW electric field strength with a factor of 2 smaller than the MW resonance method. The lower bound of the AT regime was improved from approximately 5 mV/cm to 100 μ V/cm by utilizing cold atoms to reduce the residual Doppler effect [12]. Below the AT regime where the EIT-AT splitting is indistinguishable, the MW field can be characterized by a reduction in the transparency of the probe light near the Rydberg EIT resonance [8]; however, it is not intuitive. Moreover, large uncertainties arise from temperature fluctuations, atomic density, and laser intensity. In addition, rf-dressed Rydberg atoms have exhibited enhanced DC electric field sensitivities [13]. Several rf-dressed methods have been developed to improve the limit of the minimum value of measurement below the AT regime. A heterodyne detection scenario with two electric fields of equal frequencies has been used on a cesium vapor cell to achieve a minimum detected field of 460 nV/cm [14]. Moreover, Rb vapor cells have been used to achieve fields of hundreds of pV/cm by the Rydberg-atom superheterodyne receiver based on microwave-dressed Rydberg [15]. However, such approaches require long detection times of approximately 5000 s [15] and are not intuitive.

In this work we demonstrate an auxiliary microwave field applied to Rydberg atoms that can be utilized to significantly extend the AT regime and improve the lower bound of the direct SI-traceable microwave electric field strength by two orders of magnitude in a room-temperature Rb cell with a modest setup. Contrary to a previous work of heterodyne detection [14,15], the frequency of the auxiliary microwave field is different from that of the target field by approximately 1.4 GHz. The primary objective of this study was shifting the sensor's

*fxie@tsinghua.edu.cn

†zpzhang@ucas.ac.cn

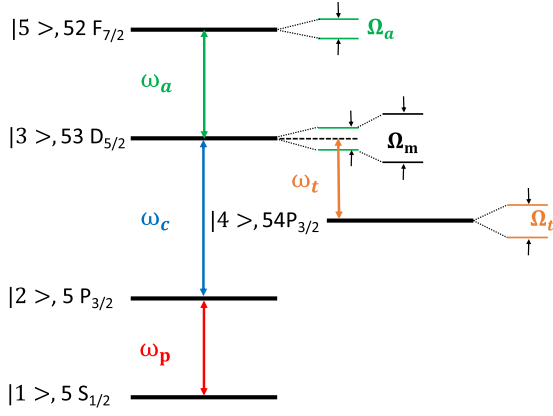


FIG. 1. Atomic energy level scheme of an auxiliary microwave-dressed Rydberg EIT and AT splitting.

span to a more sensitive area, which considerably improves the performance of quantum microwave electrometry.

II. THEORETICAL METHOD

The AT splitting of a Rydberg line under the presence of an auxiliary microwave field is employed to measure the amplitude of the signal microwave field. An auxiliary microwave field is employed to extend the range over which the microwave field can be measured to lower values. Figure 1 shows the atomic energy levels of the auxiliary microwave-dressed Rydberg EIT and AT splitting. The advance here appears to be mostly arising from a splitting the Rydberg line by a strong auxiliary field. The two “new” lines that arise are then detuned from the auxiliary-field-free transition by several MHz. The

two new lines then respond to the signal weak field in a way that is similar to a usual AC shift, in which the AC shift of the two “new lines” goes opposite ways as shown in Fig. 1. Then the EIT-AT splitting enlarged by signal microwave field is used to measure the strength of signal of the microwave field. We will explain this process from two aspects: numerical simulation and simple analytical derivation.

A. Numerical simulation

When the amplitude of the microwave field E_{MW} is sufficiently strong, the so-called AT regime, the Rydberg EIT and AT splitting Δf_m has a linear relationship with E_{MW} [8–10],

$$|E_{MW}| = \frac{\hbar}{\mu_{MW}} \Omega_{MW} = \frac{\hbar}{\mu_{MW}} D \Delta f_m, \quad (1)$$

where Ω_{MW} is the Rabi frequency for the microwave transition, \hbar is Planck’s constant, μ_{MW} is the dipole moment of the microwave atomic transition, $D = \lambda_p/\lambda_c$ is called the residual Doppler parameter for the Doppler mismatch of λ_p , and λ_p and λ_c are the wavelengths of the probe and coupling lasers, respectively. The Doppler factor D in Eq. (1) only applies when the probe light is scanned. The linear relationship in Eq. (1) does not hold when Δf_m becomes smaller than Γ_{EIT} [10].

We improve the theoretical model in the ATOMICDENSITYMATRIX package (e.g., [16,17]) to calculate the Rydberg EIT-AT [18,19], and we introduce the two-photon Rabi frequency $\Omega_{2 \times MW}$ by the perturbation method [20]. The Hamiltonian of the system under the rotating-wave approximation is given by

$$H = \frac{\hbar}{2} \begin{bmatrix} 0 & \Omega_p & 0 & 0 & 0 & 0 \\ \Omega_p & -2\Delta_p & \Omega_c & 0 & 0 & 0 \\ 0 & \Omega_c & -2(\Delta_p + \Delta_c) & \Omega_t & \Omega_a & 0 \\ 0 & 0 & 0 & \Omega_t & 0 & \Omega_{2 \times MW} \\ 0 & 0 & 0 & \Omega_a & -2(\Delta_p + \Delta_c - \Delta_a) & 0 \\ 0 & 0 & 0 & \Omega_a & \Omega_{2 \times MW} & -2(\Delta_p + \Delta_c + \Delta_t) \end{bmatrix}, \quad (2)$$

where Ω_i is the Rabi frequency, ω_i is the angular frequency of the light field, and ω_{i0} is the angular frequency corresponding to the atomic resonance transition, detuning $\Delta_i = \omega_i - \omega_{i0}$. Here, i can be p, c, t, or a, which denote the probe light, coupling light, target, and auxiliary microwave electric field, respectively. Anderson *et al.* investigated the two-photon AT splitting of $nS_{1/2}-(n+1)S_{1/2}$ and $nD_{5/2}-(n+1)D_{5/2}$ in ^{85}Rb atoms in a room-temperature vapor cell and estimated the two-photon Rabi frequency as $\Omega_{2 \times MW} \propto \Omega_1 \Omega_2 / 2\Delta$, where Ω_1 and Ω_2 are the single-photon Rabi frequencies, and Δ is the detuning of the microwave frequency from the intermediate state [20]. In our case, the detuning amount of each microwave field is caused by the dressed of the atomic energy level by another microwave field, that is, $\Delta = \frac{\Omega_a}{2} + \frac{\Omega_t}{2}$. Therefore we proposed the two-photon Rabi frequency with a fitting parameter s as $\Omega_{2 \times MW} = s \frac{\Omega_a \Omega_t}{\Omega_a + \Omega_t}$ in the H following Ref. [20]. Then the transmittance of the probe light is $T =$

$\exp(-\frac{2\pi l}{\lambda_p} \text{Im}[\Xi])$, where the susceptibility $\Xi = \frac{2N_0}{E_p \epsilon_0} \rho_{21D}$, N_0 is the atomic number density, and the subscript D represents the Doppler average of ρ_{21} [10].

Figure 2 shows the simulation results of Rydberg EIT-AT splitting Δf_m and Ω_t with several typical auxiliary microwave electric field Rabi frequencies $\Omega_a \sim 0, 0.5, 1, 2 \times \Gamma_{EIT}$. The data are calculated with $\Omega_p = 0.4 \times 2\pi$ MHz and $\Omega_c = 3.5 \times 2\pi$ MHz, which are typical parameters in the calculations and experiments [10], and $s = 2$ is chosen to exhibit two-photon resonance transition. The result with $\Omega_a = 0$ shows that Δf_m no longer satisfies the linear relationship when $\Omega_t < \Gamma_{EIT}$, and Δf_m is indistinguishable when $\Omega_t < 0.5 \times \Gamma_{EIT}$. When $\Omega_a \sim \Gamma_{EIT}$ or $\Omega_a > \Gamma_{EIT}$, it can be seen that the EIT-AT splitting always exists, and Δf_m maintains a monotonic relationship with Ω_t . The method extends the AT regime, and Δf_m can be utilized to characterize weak E_t .

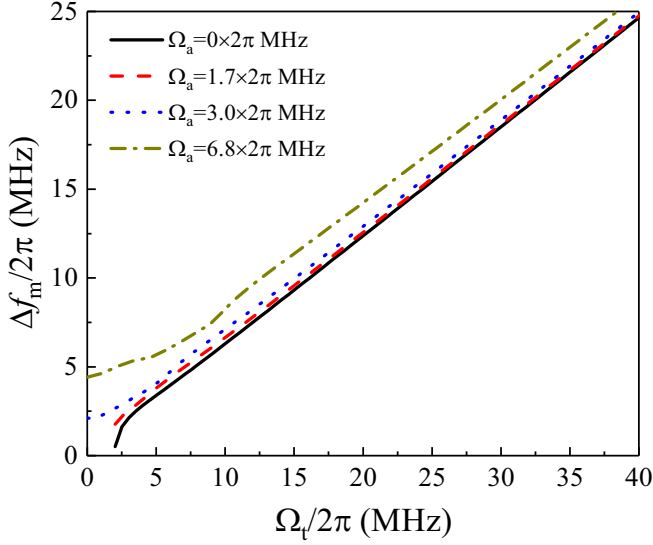


FIG. 2. Simulation results of Rydberg EIT-AT splitting Δf_m and Ω_t with different auxiliary microwave electric field Rabi frequencies. Note that the linewidth of the Rydberg EIT is $\Gamma_{EIT} = 3.5 \times 2\pi$ MHz at gas temperature 300 K.

B. Simple analytical model

Considering only the 3×3 submatrix with two microwave fields in H , the relationship between the EIT-AT splitting Δf_m and Rabi frequency of the two microwave fields can be described by an analytic expression as $\Delta_c = \Delta_a = \Delta_t = 0$ [21],

$$\Delta f_m = \frac{1}{D} \Omega_m = \frac{1}{D} \sqrt{\frac{\Omega_a^2 + \Omega_t^2 + \left(s \frac{\Omega_a \Omega_t}{\Omega_a + \Omega_t}\right)^2}{3}} \times [\cos \theta - \cos(\theta + 2\pi/3)], \quad (3)$$

where $\theta = \frac{1}{3} \arccos\left(\frac{\Omega_a \Omega_t s \frac{\Omega_a \Omega_t}{\Omega_a + \Omega_t}}{\left(\frac{1}{3} [\Omega_a^2 + \Omega_t^2 + \left(s \frac{\Omega_a \Omega_t}{\Omega_a + \Omega_t}\right)^2]\right)^{3/2}}\right)$.

The results of this analytical expression are in good agreement with those of the simulation. The relation between Δf_m and Ω_t show a nonlinearity relationship, especially at the very low field. The explanation is as follows: when two microwave fields act on the system, the EIT-AT split is not only related to the Rabi frequency of each microwave field but also Rabi frequencies of both microwave fields. When one takes the two-microwave photon interaction $\Omega_{2 \times MW} = 0$, Eq. (3) yields familiar results [21], as $\Delta f_m(\Omega_{2 \times MW} \rightarrow 0) = \frac{1}{D} \sqrt{\Omega_t^2 + \Omega_a^2}$, which is responsible for the nonlinearity relationship. When $\Omega_a = 0$, Eq. (3) attains the most common results $\Delta f_m = \frac{1}{D} \Omega_t$, as shown in Eq. (1). Moreover, the two-photon Rabi frequency $\Omega_{2 \times MW}$, which is proportional to the product of the Rabi frequencies of the two microwave fields, makes the nonlinearity more complicated.

III. EXPERIMENTAL SETUP AND METHODS

We experimentally demonstrated the above advantages in a room-temperature vapor cell of ^{87}Rb . The energy levels of ^{87}Rb , $5S_{1/2}(F=2)$, $5P_{3/2}(F=3)$, $53D_{5/2}(F=4)$, and $54P_{3/2}(F=3)$, $52F_{7/2}(F=5)$ correspond to $|1\rangle$, $|2\rangle$, $|3\rangle$,

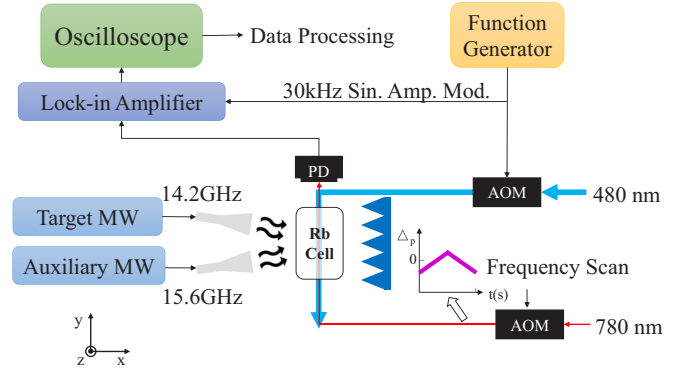


FIG. 3. Scheme of the assisted microwave-dressed Rydberg EIT-AT splitting.

$|4\rangle$, $|5\rangle$ in the theoretical model, respectively. Figure 3 shows a diagram of the experimental setup. The probe light ($\lambda_p \sim 780$ nm) is generated by a tunable diode laser (DL100, Toptica). The frequency of the laser can be scanned around the resonance transition of ^{87}Rb $5S_{1/2}(F=2)$ to $5P_{3/2}(F=3)$ with ± 25 MHz by an acousto-optic modulator (AOM) [19] in 250 ms for each measurement. The coupling light of ($\lambda_c \sim 480$ nm) is generated by a frequency-doubled diode laser (TA-SHG-Pro, Toptica), and its frequency is locked at the resonance transition of ^{87}Rb $5P_{3/2}(F=3)$ to $53D_{5/2}(F=4)$ by the Zeeman modulation method [18]. The diameter of the probe light and the coupling light is approximately $800 \mu\text{m}$ and $900 \mu\text{m}$, respectively. The intensity of the probe light and the coupling light is $60 \mu\text{W}$ and 40 mW, respectively. The intensity of the coupling light can be modulated by the AOM with a modulation frequency of 30 kHz to improve the signal-to-noise ratio of the EIT-AT spectra. The intensity of the probe light is recorded by a photodetector (PDA36A2, Thorlabs) after interaction with coupling light and microwaves in the Rb cell and then sent to a lock-in amplifier (LI5640, NF Corporation).

The two microwave fields correspond to the Rydberg transitions at $53D_{5/2}(F=4)$ to $54P_{3/2}(F=3)$ (~ 14.2 GHz) and $53D_{5/2}(F=4)$ to $52F_{7/2}(F=5)$ (~ 15.6 GHz). They are provided by the two signal sources (E8257D and 8340B, Keysight Technologies) and then irradiated to the Rb cell through two rectangular horn antennas. The horn antennas are placed far from the atom cell to meet the far-field conditions of microwave field transmission. The probe light, coupling light, and microwave fields are vertical linear polarizations (along the z axis), and the propagation of the microwave fields is perpendicular to the coupling beam and the probe beam. Note that the Rydberg EIT-AT splitting in the linear AT regime is used to calibrate E_t or E_a , and then a calibrated linear attenuator is used to obtain weak E_t or E_a [8–10].

The effect of the interference of two microwave fields can be ignored in our work for the following reasons. (1) The frequency of the difference frequency term in the interference is about 1.4 GHz. There is no related energy-level transition starting from the three Rydberg states involved in the system. Then the microwave field caused by the difference frequency term in the interference has a huge amount of detuning for the atomic energy levels in the system, and the

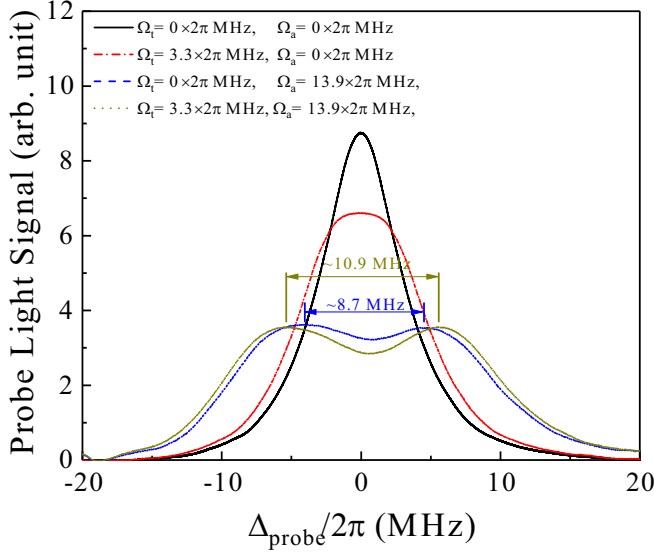


FIG. 4. An experimental example of Rydberg EIT and AT splitting spectra by an auxiliary microwave field. Black line: The Rydberg EIT signal without microwave electric field. Red line: When the target microwave electric field is too weak to generate the EIT-AT splitting. Blue line: When only the auxiliary microwave electric field is turned on, a clear EIT-AT is observed. Dark yellow line: When both the auxiliary and target microwave electric fields are turned on, the EIT-AT splitting becomes larger than those of the blue line.

influence of the difference frequency term can be ignored. And the frequency of the sum frequency term corresponds to the transitions of state $|4\rangle$ to $|5\rangle$, but the difference in the orbital angular momentum of $|4\rangle$ and $|5\rangle$ is 2, which belongs to the dipole-forbidden transition, and the probability of single-photon transition is very small and can be ignored. (2) Reference [11] reported a Rydberg-atom-based mixer to measure the phase of a radio frequency wave. Their work showed that the beat signal is almost undetectable when the frequencies of the two microwaves differ by 2.5 MHz. The frequency difference of the two microwaves in our case is about 1.4 GHz. Therefore the influence of interference between two microwave fields on the experiment can be ignored in our work.

IV. RESULTS

Figure 4 shows an experimental example of the Rydberg EIT and EIT-AT splitting spectra by an auxiliary microwave field. The Rabi frequency of the auxiliary microwave electric field is directly measured through Eq. (1). The black line is a typical Rydberg EIT spectrum. When the target microwave electric field is too weak to generate EIT-AT splitting, the linewidth of the Rydberg EIT widens with a decrease in the transmittance at the resonance, shown as a red line in Fig. 4. When only the auxiliary microwave electric field is switched on, the EIT-AT splitting is observed as the blue line shown in Fig. 4. When adding the same target microwave electric field as the red line on the basis of the auxiliary microwave electric field, the EIT-AT splitting becomes larger than that of the blue line. By using this enlarged EIT-AT splitting, the intensity of

the weak target microwave electric field E_t can be measured more conveniently and accurately.

The line shape of the green peaks shows asymmetry in Fig. 4, and the theoretical calculations show that the asymmetry of the EIT-AT spectrum should be that the positions of $|4\rangle$ and $|5\rangle$ are asymmetrical to $|3\rangle$. This causes the spectrum obtained by scanning the probe light from low frequency to high frequency to be asymmetrical with the spectrum obtained from scanning from high frequency to low frequency. But the interval of EIT-AT in the two cases are same. We get the value of the microwave electric field from the interval of EIT-AT splitting; therefore the asymmetry of the EIT-AT spectrum does not have much influence on the experimental results and conclusions. The depression between the blue line and the dark yellow line is not located at $\Delta_p = 0$. Owing to this, Δ_t or Δ_a are not strictly equal to 0 in the experiments. The experimental results show that the small detuning does not affect the relationship between Δf_m and Ω_t when $\Delta_t, \Delta_a \ll \Omega_a$. This indicates that our method is more robust against perturbations in the experimental parameters.

The linewidth of our EIT is about 5 MHz, but this is not the reason that limits our experimental measurement of Δf_m . When there is only one microwave field, whether the EIT-AT splitting can be observed is limited by the EIT linewidth, which is also the lower limit of the traditional method to measure the microwave electric field intensity using EIT-AT splitting. But our method is to use an auxiliary microwave field to generate the EIT-AT splitting first. At this time, the signal microwave field is to make the EIT-AT larger, and the measurement accuracy of this larger is no longer limited by the EIT linewidth. It is limited by the scanning step of probe frequency, laser linewidth, stationary atom EIT linewidth, and so on. In our experiment, the scanning step of the probe light frequency is set to about 1 kHz, which is determined by the AOM, which is the main limitation of accuracy limit of Δf_m .

The Δf_m corresponding to E_t are measured with $\Omega_a = 8.4 \times 2\pi$ MHz, and the results are shown in Fig. 5. The results without the auxiliary microwave field are indicated by the black hollow squares in Fig. 5, and the red line is calculated by Eq. (1). The results show that Δf_m is indistinguishable when E_t is smaller than 3 mV/cm, and it cannot be used to characterize E_t , which is similar to that reported in Refs. [9,10]. The experimental results show that Δf_m exhibits a monotonic relationship with E_t with the auxiliary microwave field, even when E_t is very small, as shown by the dark hollow yellow circle in Fig. 5. The dark yellow line is calculated with Eq. (3) by fitting $s = 2.3$, which is in good agreement with the experimental results. The minimum microwave electric field intensity measured and characterized by Δf_m can be as small as $31 \pm 15 \mu\text{V}/\text{cm}$. The green data approach the auxiliary-field-induced EIT-AT splitting (5.2 MHz here) in a quadratic fashion in the weak microwave field, which makes the readings sensitive to noise effects in measuring the splitting. In addition, any small noise can move the broad peaks in Fig. 4 by a small fraction of their linewidth. Considering this fact and the error bars in Fig. 5, and some disagreement between the calculation, the confidence level on the splitting is about 30 kHz at best in the experiment, which would set the field sensitivity at $31 \pm 15 \mu\text{V}/\text{cm}$ in our method. If a spectral resolution accuracy of 1 Hz can be achieved by narrowing

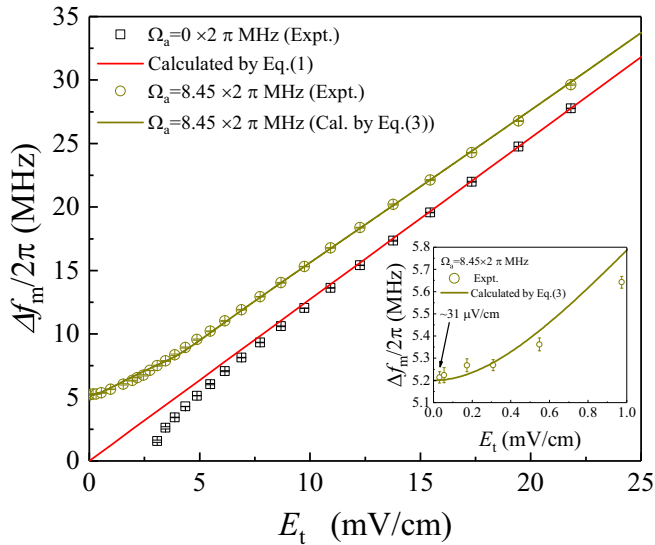


FIG. 5. Δf_m corresponding to E_t are measured with different Ω_a . The error is smaller than the icon. The inset shows an example to compare the experimental results with the calculation of Eq. (3).

the laser linewidth and reducing the laser frequency scanning step, the minimum corresponding microwave electric field can be 200 nV/cm, as predicted by our method.

V. CONCLUSION

In conclusion, we demonstrate, both theoretically and experimentally, that the EIT-AT regime and the lower bound of the direct SI-traceable electric field strength can be extended down to two orders of magnitudes lower at room temperature with a simple setup of auxiliary microwave-dressed Rydberg EIT-AT systems. The proposed method is more accurate, intuitive, and convenient than the method involving measurement of the change of probe light transmittance. Our method will greatly improve the process of quantum microwave electrometry. Furthermore, the method of first placing the sensor in the sensitive area and then measuring weak signals is suitable for extending the detection limit of other quantum sensors.

ACKNOWLEDGMENTS

This work was supported by the National Key Research and Development Program of China (Grants No. 2017YFA0304900 and No. 2017YFA0402300), the Beijing Natural Science Foundation (Grant No. 1212014), the National Natural Science Foundation of China (Grants No. 11604334 and No. 11604177), the Key Research Program of the Chinese Academy of Sciences (Grant No. XDPB08-3), and the Fundamental Research Funds for the Central Universities.

- [1] C. L. Degen, F. Reinhard, and P. Cappellaro, *Rev. Mod. Phys.* **89**, 035002 (2017).
- [2] A. D. Ludlow, M. M. Boyd, J. Ye, E. Peik, and P. O. Schmidt, *Rev. Mod. Phys.* **87**, 637 (2015).
- [3] N. Huntemann, C. Sanner, B. Lipphardt, C. Tamm, and E. Peik, *Phys. Rev. Lett.* **116**, 063001 (2016).
- [4] K. Komminis, T. W. Kornack, J. C. Allred, and M. V. Romalis, *Nature (London)* **422**, 596 (2003).
- [5] R. Mhaskar, S. Knappe, and J. Kitching, *Appl. Phys. Lett.* **101**, 241105 (2012).
- [6] J. Fang and J. Qin, *Sensors* **12**, 6331 (2012).
- [7] G. Kucsko, P. C. Maurer, N. Y. Yao, M. Kubo, H. J. Noh, P. K. Lo, H. Park, and M. D. Lukin, *Nature (London)* **500**, 54 (2013).
- [8] J. A. Sedlacek, A. Schwettmann, H. Kubler, R. Low, T. Pfau, and J. P. Shaffer, *Nat. Phys.* **8**, 819 (2012).
- [9] H. Fan, S. Kumar, J. Sedlacek, H. Kubler, S. Karimkashi, and J. P. Shaffer, *J. Phys. B: At. Mol. Opt. Phys.* **48**, 202001 (2015).
- [10] C. L. Holloway, M. T. Simons, J. A. Gordon, A. Dienstfrey, D. A. Anderson, and G. Raithel, *J. Appl. Phys.* **121**, 233106 (2017).
- [11] M. T. Simons, A. H. Haddab, J. A. Gordon, and C. L. Holloway, *Appl. Phys. Lett.* **114**, 114101 (2019).
- [12] K.-Y. Liao, H.-T. Tu, S.-Z. Yang, C.-J. Chen, X.-H. Liu, J. Liang, X.-D. Zhang, H. Yan, and S.-L. Zhu, *Phys. Rev. A* **101**, 053432 (2020).
- [13] M. G. Bason, M. Tanasittikosol, A. Sargsyan, A. K. Mohapatra, D. Sarkisyan, R. M. Potvliege, and C. S. Adams, *New J. Phys.* **12**, 065015 (2010).
- [14] J. A. Gordon, M. T. Simons, A. H. Haddab, and C. L. Holloway, *AIP Adv.* **9**, 045030 (2019).
- [15] M. Jing, Y. Hu, J. Ma, H. Zhang, L. Zhang, L. Xiao, and S. Jia, *Nat. Phys.* **16**, 911 (2020).
- [16] D. B. M. Auzinsh and S. Rochester, *Optically Polarized Atoms: Understanding Light-Atom Interactions* (Oxford University Press, Oxford, England, 2010).
- [17] S. Rochester, Atomic Density Matrix, <http://rochesterscientific.com>.
- [18] F. Jia, J. Zhang, L. Zhang, F. Wang, J. Mei, Y. Yu, Z. Zhong, and F. Xie, *Appl. Opt.* **59**, 2108 (2020).
- [19] F. Jia, Y. Yu, X. Liu, X. Zhang, L. Zhang, F. Wang, J. Mei, J. Zhang, F. Xie, and Z. Zhong, *Appl. Opt.* **59**, 8253 (2020).
- [20] D. A. Anderson, A. Schwarzkopf, S. A. Miller, N. Thaicharoen, G. Raithel, J. A. Gordon, and C. L. Holloway, *Phys. Rev. A* **90**, 043419 (2014).
- [21] P. R. Berman and V. Malinovsky, *Principles of Laser Spectroscopy and Quantum Optics* (Princeton University Press, Princeton, NJ, 2011).